DEVELOPMENT AND APPLICATION OF THE MULTIGROUP SIMPLIFIED P_3 (SP_3) EQUATIONS IN A DISTRIBUTED MEMORY ENVIRONMENT.

Gianluca Longoni, Alireza Haghighat and G. Sjoden
University of Florida
202 Nuclear Sciences Building
Gainesville, FL 32611 USA
longoni@ufl.edu; haghighat@ufl.edu; joedean@sprintmail.com

ABSTRACT

We have derived the multigroup SP_3 equations from the monodimensional P_3 equations. In this derivation we have considered isotropic source and isotropic scattering. We have eliminated the odd moments to obtain an elliptic form of the SP_3 equations. The resulting second order PDE system of equations has been discretized with a finite volume approach. The linear system of equations, arising from the discretization with the finite volume approach, is solved with LU decomposition and iterative refinement. We have developed a parallel code, namely $PENSP_3$ for solving the SP_3 equations with moment decomposition in 3-D geometry. We have estimated the accuracy of the SP_3 methodology, for criticality and fixed source problems, using the PENTRAN 3-D S_N Code System. We have also analyzed the parallel performance of the $PENSP_3$ code on the PCPEN PC-Cluster.

1. INTRODUCTION

The Simplified P_N equations have been proposed and implemented as a more accurate approach compared to the diffusion equation. The first derivation of the SP_N equations can be traced back to Gelbard[1] in the early 1960s. Recently, the methodology has been subjected to renewed interest; Pomraning[2] showed that for odd N and in an infinite homogeneous medium, the SP_N equations are a variational approximation to the one-group even-parity transport equation with isotropic scattering. Furthermore, Larsen, McGhee and Morel[3], showed that these equations are higher-order asymptotic solutions to the transport equation.

The derivation of the SP_N equations consists in replacing the first order derivatives in the monodimensional P_N equations with the gradient operator for even moments and with the divergence operator for odd moments. The main advantage of the SP_N methodology compared to the Spherical Harmonics is the number of equations involved and their implementation. The number of equations to be solved increases by $(N+1)^2$ for spherical harmonics[4], while it increases by $(N+1)$ for SP_N. Moreover, the implementation of the SP_N equations on a computer requires much less effort than spherical harmonics, and the cost of computation for the SP_N method is greatly reduced.

We have derived the SP_3 equations with isotropic source and isotropic scattering starting from the monodimensional P_N equations and by eliminating the odd moments. The resulting system of second order PDE equations has been discretized with a finite volume approach. We have implemented a LU decomposition with iterative refinement solver[5].

To take advantage of parallel computing, we have developed algorithms for processing the flux moments in parallel. For this, we have used the MPI (Message Passing Interface) library[6]. A new parallel 3-D, multigroup SP_3 code has been developed; this code is referred to as $PENSP_3$ (Parallel Environment Neutral-particle Simplified P_3). The code has been tested for both eigenvalue (criticality)

and fixed source problems. To estimate the accuracy and performance of PENSP$_3$, we used the PENTRAN 3-D parallel S_N code[7].
The remainder of this paper is organized as follows. In Section 2, we derive the SP$_3$ equations, and discuss the solver used and the implementation procedure on distributed memory architectures. In Section 3, we compare the results obtained from the PENSP$_3$ code to those predicted by PENTRAN. We also discuss the issues related to speed up and parallel efficiency. In Section 4, we give a summary and discuss the conclusions, and ongoing and future work.

2. METHODOLOGY

2.1 DERIVATION OF THE SP$_3$ EQUATIONS

We start the derivation of the multigroup SP$_3$ equations from the monodimensional multigroup P$_3$ equations (Eqs. 1), assuming isotropic source and isotropic scattering.

$$\frac{d\Phi_{1,g}}{dx}+\sigma_{t,g}\Phi_{0,g}=\sum_{g'=1}^{G}\sigma_{s0,g'\to g}\Phi_{0,g'}+\frac{1}{k}\chi_g\sum_{g'=1}^{G}\nu\sigma_{f,g'}\Phi_{0,g'}+S_{0,g} \tag{1a}$$

$$\frac{2}{3}\frac{d\Phi_{2,g}}{dx}+\frac{1}{3}\frac{d\Phi_{0,g}}{dx}+\sigma_{t,g}\Phi_{1,g}=0 \tag{1b}$$

$$\frac{3}{5}\frac{d\Phi_{3,g}}{dx}+\frac{2}{5}\frac{d\Phi_{1,g}}{dx}+\sigma_{t,g}\Phi_{2,g}=0 \tag{1c}$$

$$\frac{3}{7}\frac{d\Phi_{2,g}}{dx}+\sigma_{t,g}\Phi_{3,g}=0 \tag{1d}$$

From Eq. 1b we obtain the first moment:

$$\Phi_{1,g}=-\frac{1}{3\sigma_{t,g}}\frac{d}{dx}(2\Phi_{2,g}+\Phi_{0,g}) \tag{2}$$

And by substituting Eq. 2 into Eq. 1a, we obtain:

$$\begin{aligned}-\frac{d}{dx}D_{1,g}\frac{d}{dx}F_g(x)+\sigma_{t,g}(x)F_g &= 2\sigma_{t,g}(x)\Phi_{2,g}(x)+\sigma_{s0,g\to g}(x)\Phi_{0,g}(x)+\sum_{\substack{g'=1\\g'\neq g}}^{G}\sigma_{s0,g'\to g}(x)\Phi_{0,g'}(x)\\ &+\frac{1}{k}\chi_g\sum_{g'=1}^{G}\nu\sigma_{f,g'}(x)\Phi_{0,g'}(x)+q_{ext,g}(x)\end{aligned}, \tag{3a}$$

where

$$F_g = 2\Phi_{2,g} + \Phi_{0,g}, \tag{3b}$$

and

$$D_{1,g}(\vec{r}) = \frac{1}{3\sigma_{t,g}(\vec{r})}. \tag{3c}$$

By substituting Eqs. 1d and 1a in 1c we obtain the second order differential equation for the second moment:

$$\begin{aligned} &-\frac{d}{dx}D_{2,g}(x)\frac{d}{dx}\Phi_{2,g}(x) + \sigma_{t,g}\Phi_{2,g}(x) = \\ &\frac{2}{5}\left(\sigma_{a0,g}(x)\Phi_{0,g}(x) - \sum_{\substack{g'=1 \\ g'\neq g}}^{G}\sigma_{s0,g'\to g}(x)\Phi_{0,g'}(x) - \frac{1}{k}\chi_g\sum_{g'=1}^{G}\nu\sigma_{f,g'}(x)\Phi_{0,g'}(x) - q_{ext,g}(x)\right), \end{aligned} \tag{4a}$$

where

$$D_{2,g}(\vec{r}) = \frac{9}{35\sigma_{t,g}(\vec{r})} \tag{4b}$$

We obtain the SP_3 equations by substituting the first order derivative operator in Eqs. 3 and 4 with the gradient operator as follows:

$$\begin{aligned} &-\vec{\nabla}D_{1,g}(\vec{r})\vec{\nabla}F(\vec{r}) + \sigma_{t,g}(\vec{r})F(\vec{r}) = 2\sigma_{t,g}(\vec{r})\Phi_{2,g}(\vec{r}) + \sigma_{s0,g\to g}(\vec{r})\Phi_{0,g}(\vec{r}) + \sum_{\substack{g'=1 \\ g'\neq g}}^{G}\sigma_{s0,g'\to g}(\vec{r})\Phi_{0,g'}(\vec{r}) \\ &+\frac{1}{k}\chi_g\sum_{g'=1}^{G}\nu\sigma_{f,g'}(\vec{r})\Phi_{0,g'}(\vec{r}) + q_{ext,g}(\vec{r}) \end{aligned} \tag{5}$$

$$\begin{aligned} &-\frac{d}{dx}D_{2,g}(\vec{r})\frac{d}{dx}\Phi_{2,g}(\vec{r}) + \sigma_{t,g}(\vec{r})\Phi_{2,g}(\vec{r}) = \\ &\frac{2}{5}\left(\sigma_{a0,g}(\vec{r})\Phi_{0,g}(\vec{r}) - \sum_{\substack{g'=1 \\ g'\neq g}}^{G}\sigma_{s0,g'\to g}(\vec{r})\Phi_{0,g'}(\vec{r}) - \frac{1}{k}\chi_g\sum_{g'=1}^{G}\nu\sigma_{f,g'}(\vec{r})\Phi_{0,g'}(\vec{r}) - q_{ext,g}(\vec{r})\right) \end{aligned} \tag{6}$$

The Marshak-like vacuum boundary conditions for Eqs. 5 and 6 are:

$$\frac{1}{2}F_g(\vec{r}) + D_{1,g}(\vec{n}\cdot\vec{\nabla})F_g(\vec{r}) = \frac{3}{8}\Phi_{2,g}(\vec{r}) + \int_0^{2\pi}\int_{-1}^{0} 2|\mu|\psi^b(\vec{r},\mu,\varphi)d\mu d\varphi \tag{7}$$

$$\frac{21}{40}\Phi_{2,g}(\vec{r}) + D_{2,g}(\vec{n}\cdot\vec{\nabla})\Phi_{2,g}(\vec{r}) = \frac{3}{40}F_g(\vec{r}) + \frac{3}{5}\int_0^{2\pi}\int_{-1}^{0} 2P_3(|\mu|)\psi^b(\vec{r},\mu,\varphi)d\mu d\varphi \tag{8}$$

We discretize Eqs. 5 and 6 using a finite volume approach, and obtain two sets of linear systems of equations. The SP_3 equations are a coupled system of differential equations, with coupling occurring between the zeroth and the second moment. For this reason we use an iterative procedure to solve the equations. The first step is to solve Eqs. 5 with the second moment equal to zero. We can observe that Eq. 5 with second moment set equal to zero is the diffusion equation, hence the solution obtained from this equation is a good starting guess[4].
Subsequently, we obtain the scalar flux from Eq. 3b as

$$\Phi_{0,g} = F_g - 2\Phi_{2,g} \tag{9}$$

Once we have obtained the second moment, we update the source in Eqs. 6 and repeat the procedure until the convergence tolerance is satisfied.

2.2 DISCUSSION ON THE SOLVER FOR THE LINEAR SYSTEMS

We have implemented a matrix solver utilizing the LU decomposition method. We have parallelized on two processors the decomposition of the matrix for the zeroth and the second moment. Once the decomposition has been obtained the solution is calculated by forward elimination and backward substitution with iterative refinement. With the iterative refinement technique it is possible to avoid the accumulation of round-off errors occurring with direct methods of solution, especially when the matrix is close to singular[5].
The iterative improvement of the solution is achieved in a very straightforward manner. Given **x** is the exact solution of the linear set

$$Ax = b \tag{10}$$

Although the solution **x** is not known, we only have a slightly wrong solution **x+δx**, where **δx** is the unknown error. If the matrix **A** multiplies this solution, we obtain a right hand side that is discrepant from **b**.

$$A\cdot(x+\delta x) = b + \delta b \tag{11}$$

If we subtract Eq. 10 from Eq. 11, we obtain

$$A \cdot \delta x = \delta b \tag{12}$$

By substituting Eq. 12 into Eq. 11, we can solve for **δx** . By subtracting this error from the wrong solution **x+δx**, we obtain an improved solution.

2.3 IMPLEMENTATION ON DISTRIBUTED MEMORY ARCHITECTURES

The PENSP$_3$ code has been implemented on distributed memory architectures using the MPI parallel libraries. At this stage of development, we have performed moment decomposition on two processors. The PENSP$_3$ code distributes the arrays containing the matrices for the zeroth and second moment to two separate processors. The solution for each moment is computed, and at each iteration the information is exchanged between the two processors. As we will show in Section 3, this type of decomposition provides good speedup and parallel efficiency. The LU decomposition of the matrices is also distributed on two processors. The parallel computer utilized is the PCPEN[a] cluster. The system has 8 processors, with 2 GByte RAM each. The head node is an Athlon Pentium IV 1.6 GHz and the remaining 7 nodes have Pentium III 1 GHz processors.

3. RESULTS

We have tested PENSP$_3$ for criticality and fixed source problems, and compared its results to those obtained with PENTRAN.

3.1 PROBLEM 1

The first problem considered is a criticality (eigenvalue) problem obtained from Ref. 4. The mesh and material distribution are shown in Fig. 1.

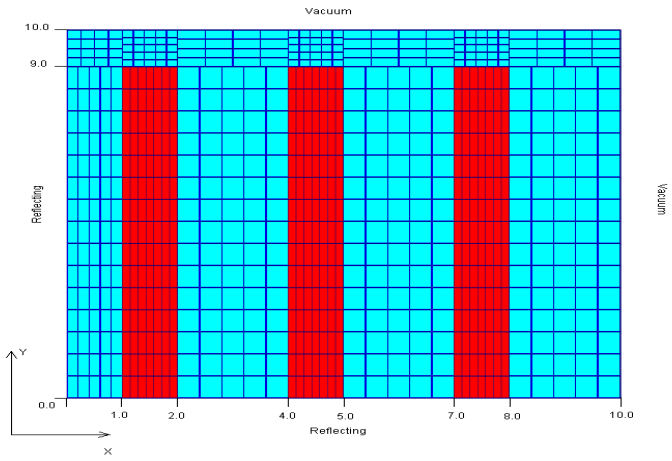

Figure 1. Mesh and material distribution for the eigenvalue problem (dimensions in cm)

In Fig. 1, the red regions represent the fuel, while the cyan regions present the moderator. A one group, P0 scattering cross section set, given in Table I, is used for this example.

[a] Part of the Particle Transport and Distributed Computing Laboratory at the University of Florida.

Table I. Eigenvalue problem P0 cross sections

Material	σ_a	$\nu\sigma_f$	σ_t	σ_{s0}
Fuel	0.15	0.24	1.5	1.35
Moderator	0.07	0.0	1.0	0.93

We compared the results obtained by $PENSP_3$ with the PENTRAN S_N code; in Table II we show the results for different S_N orders and the relative difference between the two codes.

Table II. Comparison of results between $PENSP_3$ and PENTRAN S_N code.

Methodology	k eigenvalue	Relative difference[b](%)
$PENSP_3$	0.80197	Reference
PENTRAN S_{16}	0.80092	0.13
PENTRAN S_{18}	0.80099	0.12
PENTRAN S_{20}	0.80107	0.11

$$b)\frac{k(PENSP_3)-k(PENTRAN)}{k(PENTRAN)}\times 100$$

The results obtained for the k eigenvalue are in good agreement with those given in Ref. 4. Besides the k values, the flux distributions are also in good agreement. Figs. 2a and 2b show the comparison of fluxes at two y positions.

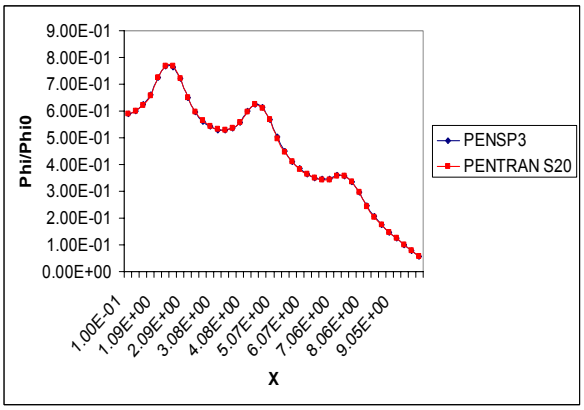

Figure 2a. Critical flux distribution (normalized) at y=4.5 cm

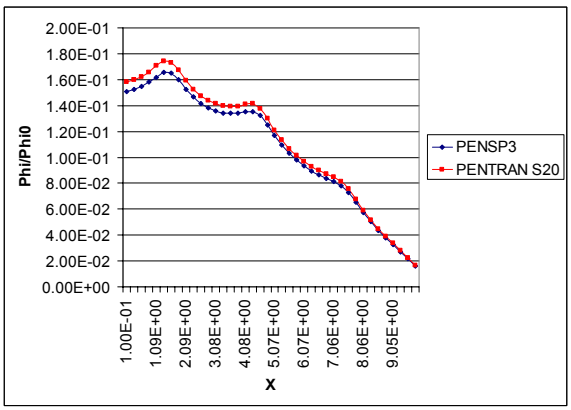

Figure 2b. Critical flux distribution (normalized) at y=9.0 cm

The maximum relative differences are 1.5% and 5% for y=4.5 cm and y=9.0 cm, respectively.

3.2 PROBLEM 2

This problem involves the eigenvalue calculation for a critical assembly of highly enriched ^{235}U (enrichment=93.2%) surrounded by water. The x-y material and mesh distribution is shown in Fig. 3. The model consists of one z-level ranging from z=0.0 cm to z=12.0 cm (discretized to 15 z-fine meshes), and placed in vacuum.

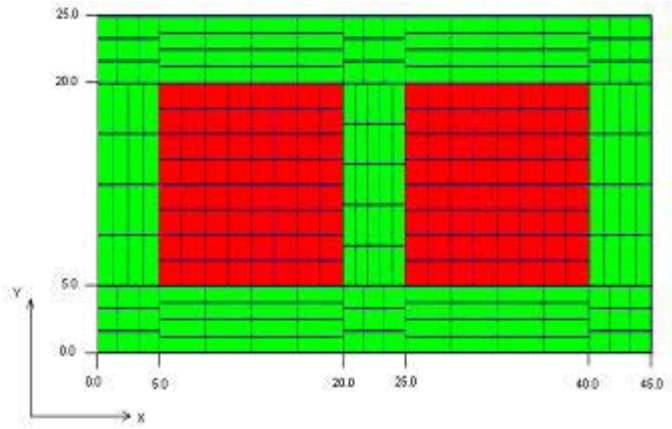

Figure 3. Mesh and material distribution for the critical assembly (dimensions in cm)

We collapse the Hansen-Roach cross-section library to two groups for fast assembly calculations with P0 scattering expansion, as presented in Table III.

Table III. Critical assembly 2 groups P0 cross sections

Material	Group	σ_a	$\nu\sigma_f$	σ_t	$\sigma_{s,g\to g}$	$\sigma_{s,g'\to g}$	χ
U-235	1	6.1902e-2	1.4436e-1	2.3968e-1	1.5220e-1	0.0	0.896
	2	8.6126e-2	1.7309e-1	4.2551e-1	3.3938e-1	2.5582e-2	0.104
Water(H_20)	1	1.9704e-4	0.0	2.8199e-1	1.5257e-1	0.0	0.0
	2	9.5040e-3	0.0	1.9796e0	1.9701e0	1.2922e-1	0.0

Figs. 4a and 4b, shows the x-y fast and thermal flux distributions at z=6.0cm, calculated by $PENSP_3$.

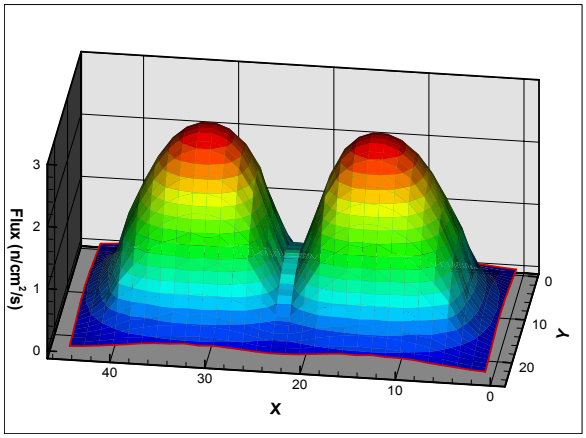

Figure 4a. Fast flux distribution at z=6.0 cm

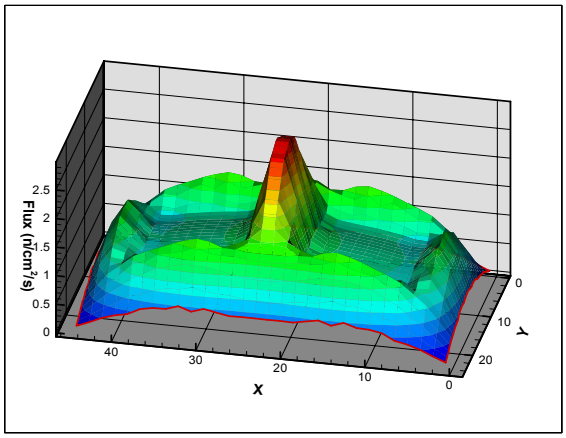

Figure 4b. Thermal flux distribution at z=6.0 cm

In Figs. 5 and 6, we compare the critical fluxes for the fast and thermal energy groups at y=12.5 cm z=6.0 cm. These results demonstrate excellent agreement between the $PENSP_3$ and PENTRAN (S_8) calculations.

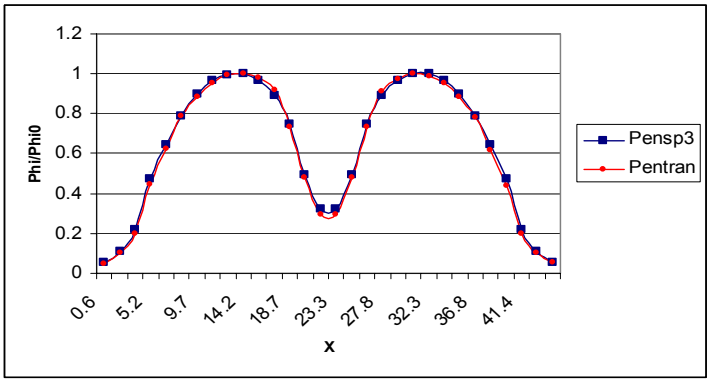

Figure 5. Critical Flux (normalized) for Fast Group at y=12.5 cm z=6.0 cm

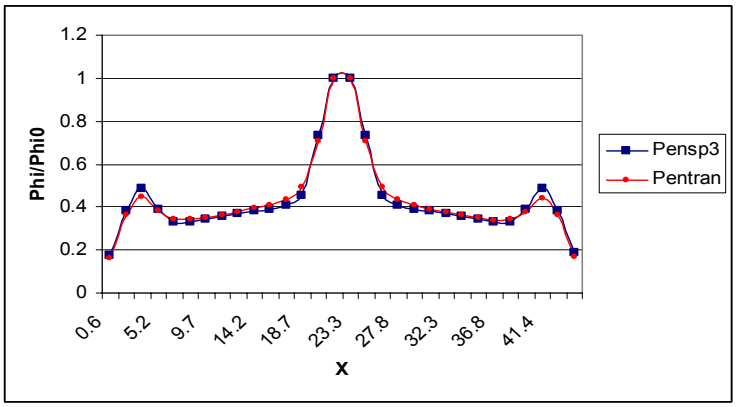

Figure 6. Critical Flux (normalized) for Thermal Group at y=12.5 cm z=6.0 cm

To maintain that the S_N order considered is adequate for PENTRAN calculations, we performed several serial calculations for S_N orders between S_8 and S_{20}. These results are summarized in Table IV.

Table IV. Analysis of the k eigenvalue as a function of the S_N order

S_N Order	k eigenvalue (PENTRAN)	Computational Time (sec)
8	1.12235	638.7
10	1.12342	783.4
12	1.12393	1080.3
14	1.12426	1372.2
16	1.12448	1972.5
18	1.12461	2707.2
20	1.12474	2725.1

Table IV indicates that PENTRAN with a S_8 quadrature set yields an accurate solution, compared to PENTRAN S_{20} (within 0.22%) considering the computational cost. The k eigenvalue obtained with $PENSP_3$ is equal to 1.15583, with a relative difference equal to 2.76% compared to PENTRAN S_{20}.
In Table V, we show the computational time for serial and parallel $PENSP_3$ calculations. A parallel efficiency of 88.8% is achieved; the loss of parallel efficiency can be attributed to the necessary communication between the two moments and relatively lower parallel fraction of the LU decomposition section which consumes a significant fraction of time, e.g., for this problem this fraction is ~34%.

Table V. Critical Assembly - Parallel $PENSP_3$ (Moment decomposition on 2 processors)

Computational Time for Serial Calculation (sec)	Computational Time for Parallel Calculation (sec)	Speed Up	Efficiency (%)
587.4	330.5	1.77	88.8

3.3 PROBLEM 3

The purpose of this fixed source-shielding problem is to test the accuracy of the SP_3 methodology as a function of the scattering ratio c is given by

$$c = \frac{\sigma_s}{\sigma_t} \tag{13}$$

This problem is a 3-D box with a source placed in its central region. Fig. 5 shows the material distribution for the model which is partitioned into two axial slices (i.e. z-levels) with each level containing 4 coarse meshes. For this study, we further partition each coarse mesh into 8x8x8 fine meshes.

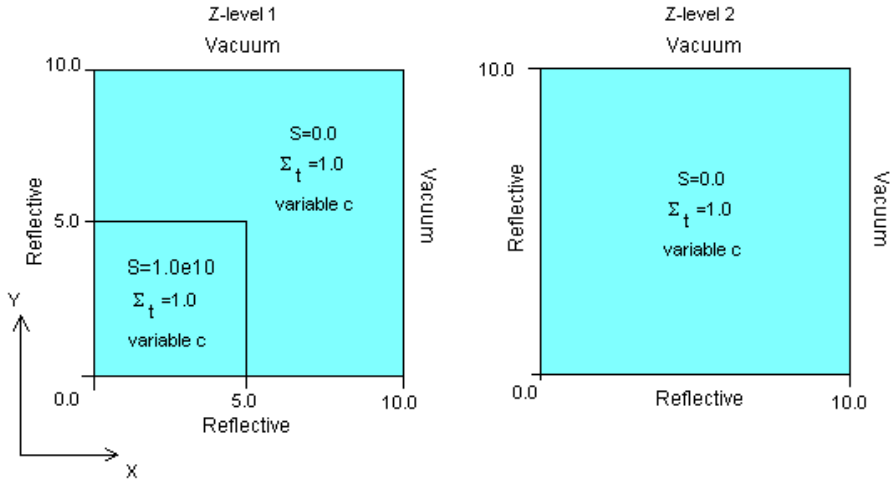

Figure 5. 3-D Box Model (dimensions in cm)

In Figs. 9 and 10, we compare the flux distributions determined by $PENSP_3$ and PENTRAN S_{20} along the x-axis for c=0.97, at the same axial level (z=5.0 cm) for two y positions of 1.0 cm and 9.0 cm, respectively.

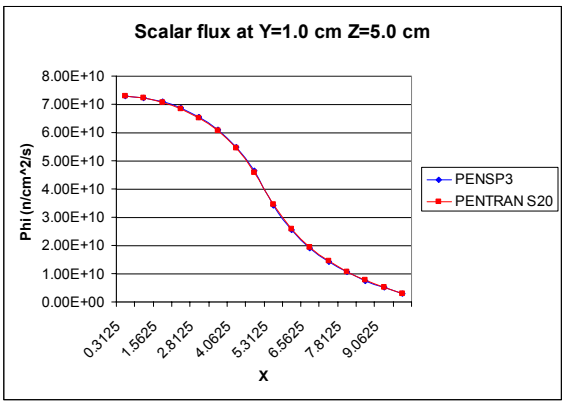

Fig. 9. Scalar flux at Y=1.0 cm and Z=5.0 cm

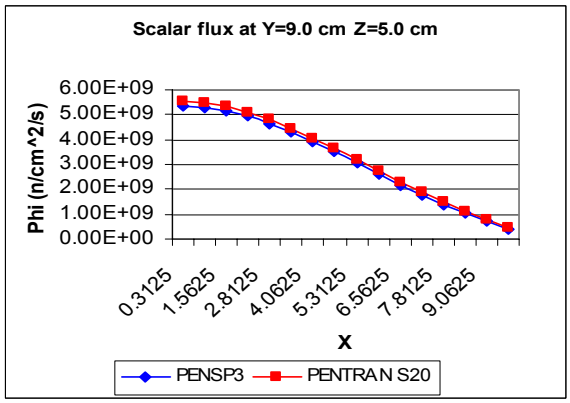

Fig. 10. Scalar flux at Y=9.0 cm and Z=5.0 cm

These results indicate that $PENSP_3$ solutions are in good agreement with the higher order S_N calculations. Even at ~7 mfps away from the source and adjacent to a vacuum boundary (using Marshak condition), the relative difference is <5%. In order to measure the effectiveness of the SP_3 formulation for problems with low c ratios (i.e., high angular dependencies), we vary the c in a range of 0.97 to 0.5. Fig. 11 shows the maximum relative difference between the $PENSP_3$ and PENTRAN calculations, for different c ratios. The relative differences are calculated at x=8.21 cm, y=5.0 cm, z=9.5 cm and x=8.71 cm, y=5.0 cm, z=9.5 cm. Again these positions were selected because they are several mfps away from the source and adjacent to the vacuum boundary. As expected, as the c ratio decreases especially in the vicinity of the vacuum boundary, the accuracy of $PENSP_3$ decreases, but this may not be important considering the magnitude of the flux is very low.

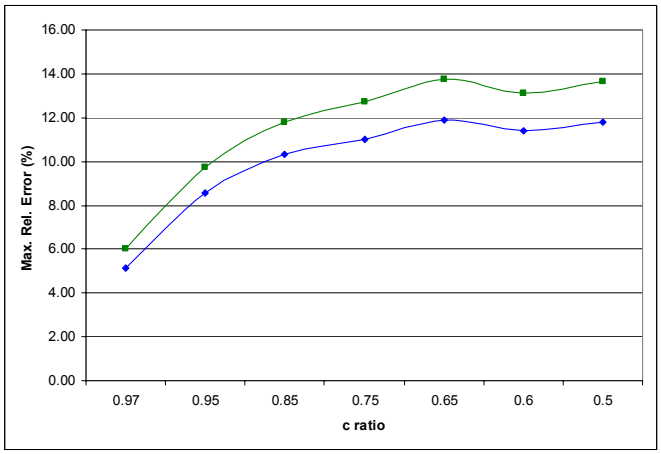

Fig. 11. Maximum relative error at different positions for different c ratio

Finally, $PENSP_3$ shows parallel efficiencies in a range 95%-98% for different c ratios.

4. SUMMARY AND CONCLUSION

We have developed a new 3-D parallel multigroup SP_3 code referred to as $PENSP_3$ (Parallel Environment Neutral-particles Simplified P_3). We have tested $PENSP_3$ for criticality and fixed source

problems. The code provides solutions that are in very good agreement with high order (N=20) S_N predictions for both criticality and shielding problems. For parallel processing, we have considered moment decomposition strategy. Our tests have demonstrated that $PENSP_3$ has excellent parallel efficiencies in a range of 89-98% for both eigenvalue and shielding problems.
One of the finding of this study is that the LU decomposition process requires significant amount of time, and cannot be parallelized as efficiently as the rest of $PENSP_3$, hence, we are investigating the use of other techniques such as the conjugate gradient. Also, since $PENSP_3$ solutions are in good agreement with the S_N predictions, we are investigating the use of $PENSP_3$ for the acceleration of the S_N method.

REFERENCES

1. E. Gelbard, J. Davis and J. Pearson, "Iterative Solutions to the P_l and Double-P_l Equations", *Nuclear Science and Engineering*, **5**, pp. 36-44 (1959).
2. G. C. Pomraning, "Asymptotic and Variational Derivations of the Simplified P_N Equations", *Ann. Nucl. En.*, **20**, pp.623 (1993).
3. E.W. Larsen, J.M. McGhee and J.E. Morel, "The Simplified P_N Equations as an Asymptotic Limit to Transport Equation", *Trans. Am. Nucl. Soc.*, **66**, pp. 231 (1992).
4. P.S. Brantley and E.W. Larsen, "The Simplified P_3 Approximation", *Nuclear Science and Engineering*, **134**, pp.1-21 (2000).
5. L.W. Johnson and R.D. Riess, *Numerical Analysis*, Addison-Wesley, Reading MA.
6. W. Gropp, E. Lusk and A. Skjellum, *Using MPI: Portable Parallel Programming with the Message-Passing Interface*, The MIT Press, Cambridge Massachussets.
7. G. Sjoden and A. Haghighat, "PENTRAN, a 3-D Scalable Transport Code with Complete Phase Space Decomposition", *Transaction of the American Nuclear Society*, **74**, pp. 181-183 (1996).